POWDER SPREAD FLAWS IN POLYMER LASER SINTERING AND ITS INFLUENCES ON MECHANICAL PERFORMANCE

Helge Klippstein[1], Hans-Joachim Schmid[1]

[1] Direct Manufacturing Research Center, Paderborn University, Germany

Contact: Helge.Klippstein@dmrc.de

Abstract

By monitoring the recoating process within polymer laser sintering production, it was shown that multiple powder-spread-flaws can be detected. Those groove-like flaws are expected to be the result of agglomerates jamming between the recoater and the last powder layer. This work is analyzing the interaction between powder-spread-flaws and part properties, showing the influence of the recoating process on the performance of laser sintering parts. Therefore, artificial powder-spread-flaws are applied to the build jobs of tensile test specimens which are measured and analyzed regarding the elongation at break, strength and fracture position. For the characteristics of the flaws, the artificial grooves are varied in depth and width. Furthermore, the position of the flaw is changed form mid part to close to surface areas. It was shown, that several flaws are visible at the part surface, resulting in stress concentration and reduced performance. But there are as well parts with flaw-layers, which are not visible after the build process on the part. Those parts can have significantly reduced mechanical properties as well.

Introduction

The part properties of laser sintered polymer components are influenced by several factors. The most prominent aspects are the powder and raw material quality [1, 2], the machine hardware and software, as well as the individual part temperature histories [3], e.g. based on the build job layout, orientation as well as cooldown times. Those influences are known and mostly understood in principle. Still the prediction of the part properties is often very complex or not possible as a lot of required data are missing. Furthermore, the mechanical properties do not only variate within one build job, e.g. related to the part position, but also from build job to build job, comparing the same positions. Especially some parts do perform very low in the elongation at break, without known explanation so far [4].

It is expected, that a milestone towards proper part performance prediction is linked to proper in-situ monitoring of the process. Multiple monitoring systems do concentrate on the build chamber temperature, which is known to have a significant influence on the part performance. Monitoring the exposure process is promising as well. Correlation of individual part temperature histories during the exposure process with the fracture position or the mechanical properties were made, but could not exclude additional other influences [5, 6]. Thus, a look into other process steps are required.

In previous work a powder spread monitoring system was developed and integrated to an EOS P395 machine at the DMRC [7]. With the monitoring system it is possible to detect powder spread flaws within every layer and link the position of the flaw to specific parts. In the following the cause of powder spreading flaws and their influence on the mechanical part properties are investigated.

There are several types of powder spreading flaws, reaching from point flaws, to line flaws and area flaws. The most common flaw is the line flaw [7], which is followed by point flaws. Area powder spread flaws do mostly build up over several layers, hence they are generated out of some line or point flaws. Or those flaws are based on a shortage of powder feed, which could be detected with our monitoring system beforehand and therefore could be prevented. As area powder spread flaws are of reduced importance, this investigation is concentrating on line flaws in form of grooves and will handle point flaws only briefly.

The origin and emergence of powder spread flaws has not been observed in detail, yet. Detectable is the result as a groove or a pile of powder on the powder bed. However, the emergence of those flaws is based on assumptions.

The point flaw: There are two different types of point flaws, the powder pile and the foreign object. Foreign objects could be char particles, which get detached from the polymer vapor coated walls of the build chamber. In a worst-case scenario, those particles do fall into the melt of an open part and might even be visible at the outer surface of those parts as can be seen in Figure 1, where this described flaw has been provoked. But single particles in comparable size have been detected several times even unprovoked.

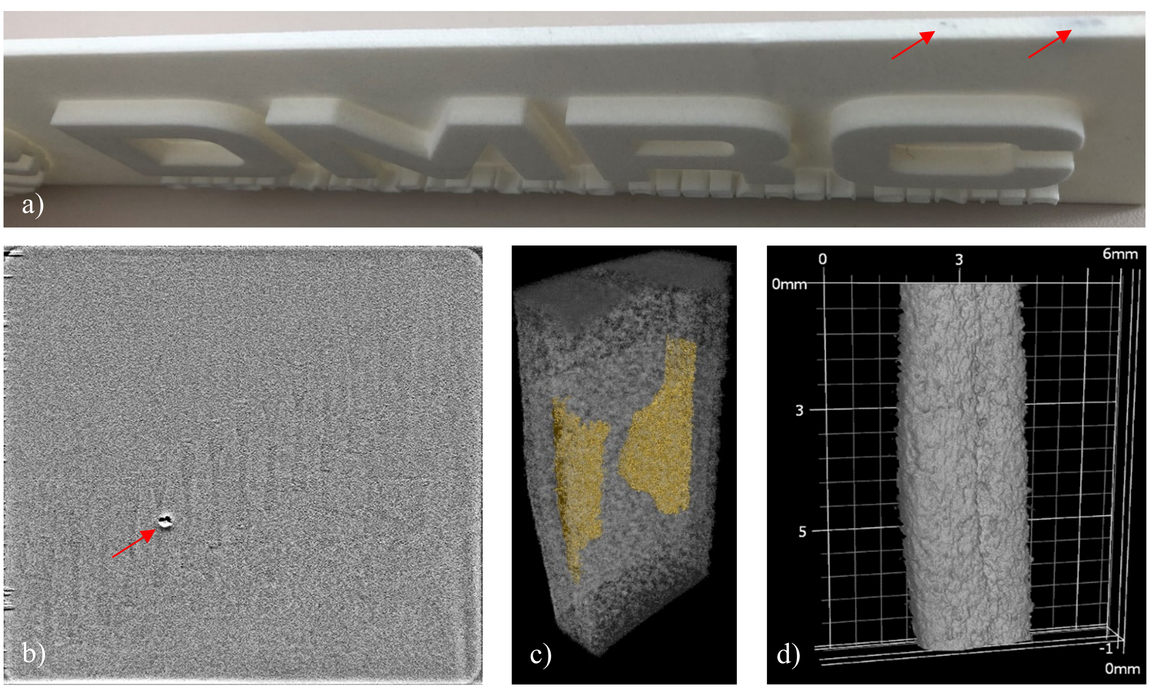

Figure 1 Point flaws: a) Char particle, visible at the outer surface of a part; b) Powder spread monitoring image of a powder pile ; c) X-CT scan of the influenced specimen; d) Surface topology of the influenced specimen (side view on the dog bone) [7]

Powder piles are often very small and can be expected to be mostly irrelevant for the part performance. However, at some point the amount of powder can be large enough, as shown in the monitoring detection image of Figure 1 b, and might lead to a delamination within a part. The delamination can be shown by X-ray computer tomography. In Figure 1 c, the pore is presented in yellow. In image d, the side surface of the specimen is shown as model generated by the fringe light *3D measuring macroscope VR-3100* from *Keyence*. The flaw is already visible on the part surface, which could even be seen by the bare eyes. [7]

The line flaw: Those flaws can be detected in one layer only (Figure 2 a) or repeatedly over several layers at the same position (Figure 2 b). Most of the grooves are starting from outside the platform and end somewhere between the left and the right platform limits. When they go all the way over the build platform, it is very likely, that the flaw can be detected in the next layer of the same recoating direction again. Thus, some flaws are visible in every odd or every even layer number. The EOS P3 system is using a recoater cassette with two recoating blades, where only one of the blade is applying the powder on the build platform per recoating direction. Hence, it can be expected, that the line flaw is linked to the left or the right-hand blade of the recoater cassette.

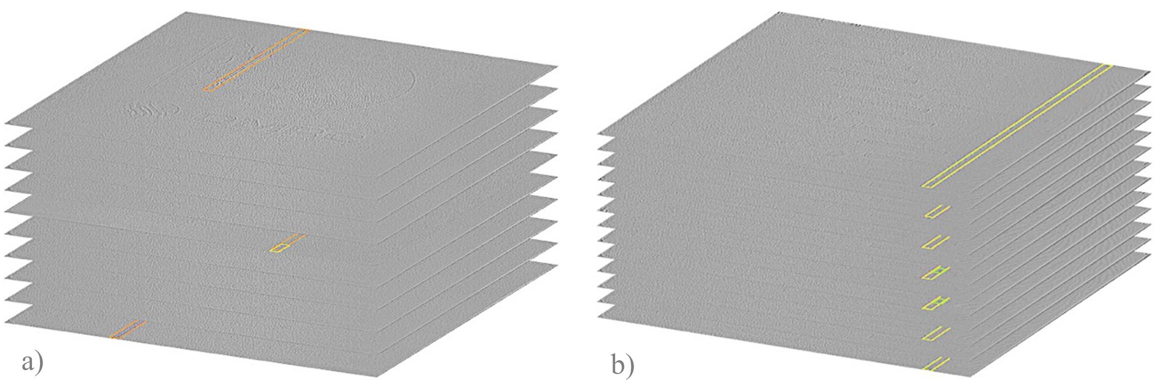

Figure 2 Line recoating flaws: a) with random, mostly short appearance; b) - with frequently position fixed appearance

It is assumed that grooves are related to agglomerates, which get stuck at the recoater blade and are pushed over the powder bed as shown in Figure 3. The formation of the agglomerates can have several causes. Polymer deposits or debris on the recoater blade might lead to some particles getting attached to the recoater for multiple layers and causing the disturbance during the recoating process. It is expected, that this leads to repeated powder spread flaws.

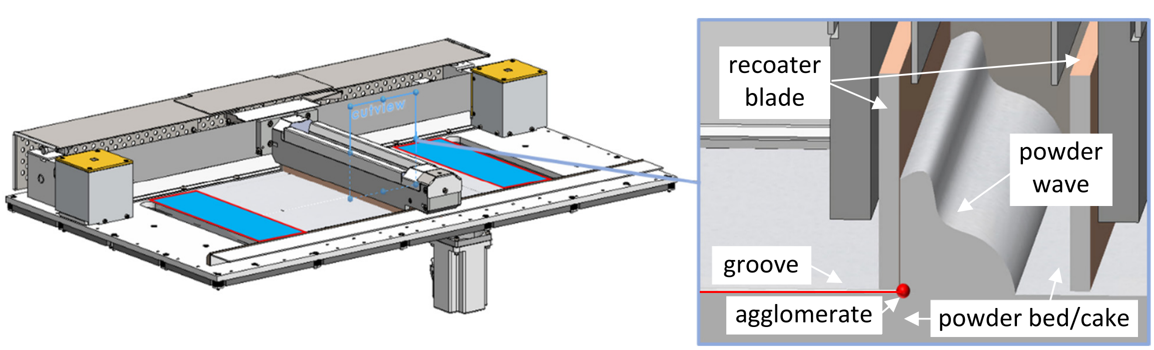

Figure 3 Groove formation due to agglomerates get stuck on the recoater

Agglomerates, which might be existing in the powder just from the beginning or are formed during the process are expected to show a more random appearance. Those agglomerates might be formed during the powder handling by refilling the machine or due to particle melt interaction when the powder wave is moving above a part area. Furthermore, the interaction of the powder with the prerun areas, which are the areas left and right between the refilling position and the build platform (light blue areas marked in Figure 3.

Even if the origin of those flaws or agglomerates is not known for sure, the groove as a result can be detected. Figure 4 shows the line flaw part interaction in a simplified model as cross section view perpendicular to a groove. The depth of a line flaw variates a lot. But when the flaw is not leading to a job termination, it can be expected, that it does not go down to the melt of the part. The powder bed thickness above a part melt pool (Figure 4 variable: r) is the sum of the layer thickness (Figure 4 variable: t) plus the sunk-shrinkage (Figure 4 variable: s) of the part, as shown in equation I. It is known that the adhesive forces work within the polymer melt, leading to a sharply rising sidewall, which in turn is the reason for the edgy upper surface properties (upskin) of laser sintering parts.

$$r = t + s \qquad \text{I}$$

$$E_{vol} = \frac{P_L}{d_H \cdot v_L \cdot t} \qquad \text{II}$$

$$E_{real} = \frac{P_L}{d_H \cdot v_L \cdot r} \qquad \text{III}$$

By calculating the volumetric energy density E_{vol} (equation II) it can be seen, that the real layer thickness r has no influence in the equation. However, by replacing the simplified layer thickness t with the real layer thickness r, the actual volumetric energy density E_{real} can be derived (equation III). Normally, the differentiation between E_{vol} and E_{real} is not required, as this equation is only used for comparing different exposure strategies. However, when the laser is melting the material of the freshly applied layer, there is an energy density peak at the position of the groove, as the real layer thickness r decreases. Additionally, this leads to an increased volume influenced by the laser within the part. It is expected, that very small grooves do not influence the melt pool, but if the groove is big enough, the melt pool will not smooth out. This might lead to a higher real layer thickness in the next layer (r^{+1}_{groove}), which in turn leads to a volumetric energy density reduction above the groove.

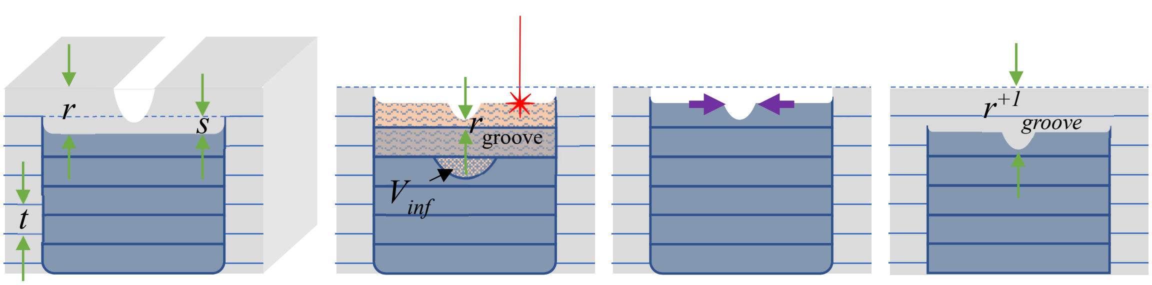

Figure 4 Schematic groove formation above a part in cut view

Theses and Experimental Set Up

The influence of the groove on the mechanical part properties shall be investigated and answer the following theses:

1. If the groove is large enough, the melt is not flowing together properly, a weakness is generated as described above. If this theory is correct, it can be expected, that the part will fail at the groove position.
2. The part orientation does influence the sensitivity of the part reacting to powder spread flaws with reduced mechanical properties. Due to the increased ratio of the flaw area to the part melt pool area in the upright specimens, compared to flat specimens, the assumption could be made, that the flaw lead to an increased performance loss for Z specimens.
3. The flaw position within the part does influence the part performance. If the flaw is visible on the part surface, it might lead to a jump in the cross section area and result in stress concentration. This can be tested, by changing the flaw position in a flat oriented specimen. The position bottom layer, mid part and upper layer shall be investigated.

The investigations have been performed on a EOS P395 laser sintering system with a self-developed powder spread monitoring system. The system can be easily retro-fitted into a standard commercial P39X system and is based on a camera mounted above the process chamber allowing to take bird view images of the fresh powder spread. A light source is located in front of the door, which increases the intensity of the shadow, casted by powder spread flaws. Those contrasts can be detected by a Mask-RCNN (Region Based Convolutional Neural Networks) software, which does the image segmentation for the powder spread flaw on the build platform. Thus, the operator gains the knowledge of the flaw position, the layer impacted as well as the parts influenced. [7]

For all investigations presented here a simple device is mounted to the recoater, which allows to apply artificial powder spread line flaws at arbitrary positions and with adjustable intensities. This system is depicted in Figure 5 and is assembled to the recoater of the P395 machine. The position can be adjusted with a precision track and carrier. On the carrier a magnet is assembled to a cantilever which can be deflected and adjusted by a precision 120 µm pitched single start screw. Via the overflow slots, it is possible to attach a pin on the magnet. This pin is then moving behind the recoater and generates a groove upon the powder bed within the freshly applied powder.

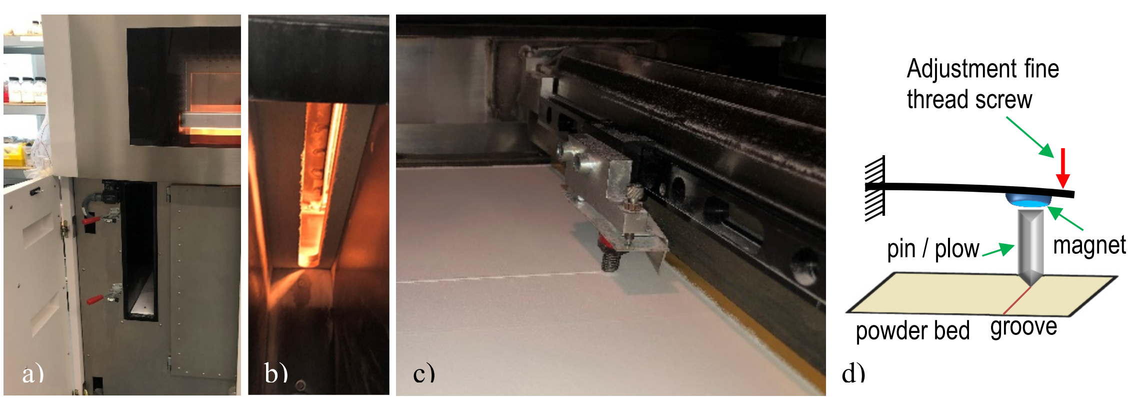

Figure 5 presentation of the flaw generation: a) EOS P395 machine with removed overflow bins; b) overflow slots at preheating phase with the recoater on the opposite side; c) artificial groove application system; d) schematic sketch of the cantilever

Experiments have shown that the pin geometry is very important for the groove geometry. The natural flaw is expected to be caused by an agglomerate, which get stuck before the recoater. Therefore, the recoating blade is leveling the left- and right-hand side of the groove.

By using a simple pin, which is attached behind the recoating blade, this leveling does not take place and the material is plowed out of the groove. Hence, there are material accumulations and small piles next to the groove as shown in

Figure 6. By using a plow pin this effect can be reduced and the piles and material next to the groove is more homogeneous. All grooves have been analyzed with the Keyence 3D measuring macroscope VR-3100 at a 40x magnification. The natural groove shows in this case the smallest severity with a depth of approximately -80 µm. The artificial pin groove has an approximated depth of -160 µm with side piles (ridge) up to 180 µm. The shown groove made with the plow is approximately -120 µm deep and the ridges are on level 90 µm.

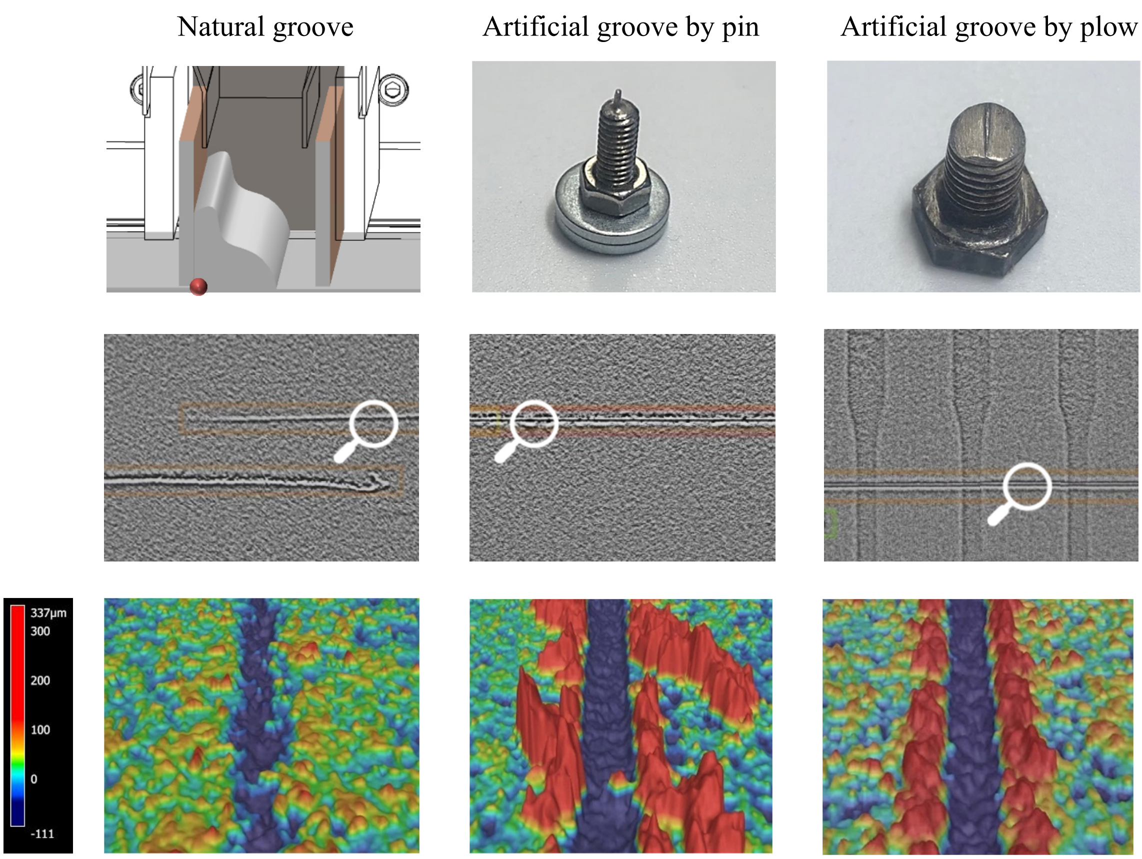

Figure 6 Comparison of natural and artificial powder bed grooves: first row the groove generators are presented, second row the monitoring data are shown, third row fringed light surface topology images

The analysis is based on tensile tests following DIN EN ISO 527 with the specimen type 1BA (cross section of 2 mm x 5 mm) with elongated shoulders to prevent slippage in the clamps of the testing machine. Compared to the type 1A specimen (cross section of 4 mm x 10 mm), it is expected that the groove is more severe in relation to the cross-section area, leading to a better groove fracture correlation. All tests have been performed on a Instron 5569 with a 5 kN load cell at 22°C. The specimens have been tested in dry condition, as they have been stored after unpacking in closed bags with silica pads. The test velocity was set to 25 mm/min.

For the analysis two different build jobs layouts (compare Figure 7) had been manufactured several times to gain in total 26 test sets with 10 specimens. For each set an artificial groove was applied within the manufacturing process and 10 reference specimens, which have been positioned as close as possible to the flaw-specimen, are build and tested to get comparable results for the mechanics. For testing only five ref-specimens and five flaw-specimens have been used to have some remaining for more in depth analysis in the future, as e.g. X-ray computer tomography.

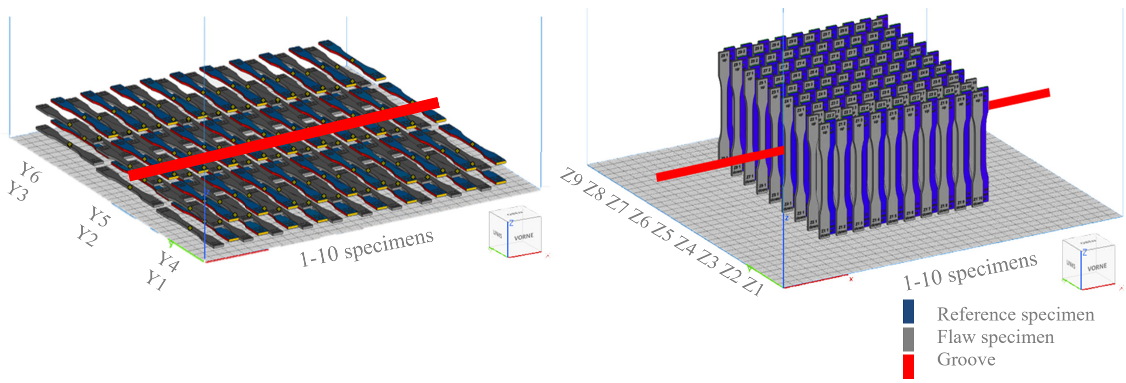

Figure 7 Test build job layout with Y oriented specimens and Z oriented specimens

All build jobs have been built with the same powder, which is a PA2200 material purchased from EOS. The powder is mixed in the ratio of 50/50, whereby the melt volume flow rate was measured with a Zwick extrusion plastometer Mflow to 37,60 cm^3/min (pre-dried material: 4.0 g; test load: 5 kg, test temperature: 235°C). The build temperature was set to 179°C and all parts were built with the 120 µm EOS part property profile at standard EOS exposure settings. The pin could be operated manually via the left bottom front door since the overflow bin has been removed (see Fig. 5a). It was expected, that by installing the overflow bin back in position the process gets more disturbed, than by leaving it open for the full build job, as by installing the bin. The air is pressed through the overflow slots into the process chamber. By having it open for the full build job there is a slight influence on the part temperature and the cool down phase on the left-hand side. However, this effect is kept constant for all build job and is expected to not influence the results, as the part position influence is not analyzed in this work.

After testing all specimens fracture positions were measured with a caliper gauge as shown in Figure 8 from the lower end of the part to the fracture position. In the same way the groove positions were measured using imageJ to determine the position of the groove related to the sample size. For the Z-oriented specimens the layer number of the groove is taken as position reference and multiplied with the layer thickness.

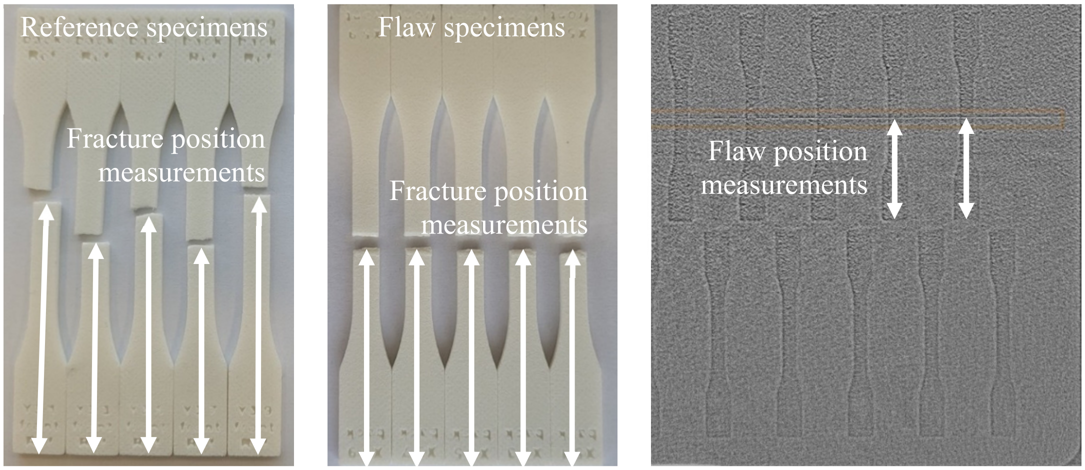

Figure 8 Fracture position measurement after tens

Those measurements do show some influences, which cannot be compensated or determined exactly, thus must be considered as measurement imprecisions:

- Plastic deformation of the specimens
- Material shrinkage and scaling factors
- Variation of the temperature distribution within the build platform
- Overcure for the Z oriented specimens (theoretical vs. real layer thickness)
- Irregular fractures
- Groove thickness of up to 1.5 mm
- Measurement inaccuracy (caliper accuracy)

To overcome this imprecisions, grooves and fracture position, which are within the same range of ±1,5 mm, are expected to be a good correlation. Hence, the artificial flaw is expected to be responsible for the fracture of the part and most probably has weakened the component significantly.

Measurement Results

For each orientation six different flaw sets have been selected for comparison. In Figure 9 the difference between the groove and fracture position is plotted over the specimen set names of exemplary selected flaw parts. There is always an image of the detection system zoomed in on the flaw and one affected part. If possible, as well the position of the flaw related to the part is given, e.g. for Y oriented specimens it is shown, if the flaw is in the middle of the part, in the first layer or last layer. Additionally, the score given by the system for the severity is given. However, this score has to be interpreted with caution.

In Y direction, the correlation of all sets with visible marks on the part upskin surface show a good correlation between the fracture and groove position. Specimen set Y4 has as well a visible mark on the part surface. As this mark is on the down skin, hence the groove was applied in the very first layer of the part the specimen cross section increases here and no specimen has broken at this position. The very light grooves of set Y5 and Y6 seem to have no influence on the fracture position. For Y6, no visible marks on the part surface or flaw detections do indicate the very small variance in fracture positions ~20 mm above the groove. Even the reference set, which is positioned 2 mm higher in the build job shows fractures at the same position. The exact reason is unknown, it can only be assumed, that there might be a heating or exposure issue for this period of time and position. In the reference specimens no anomalies have been found.

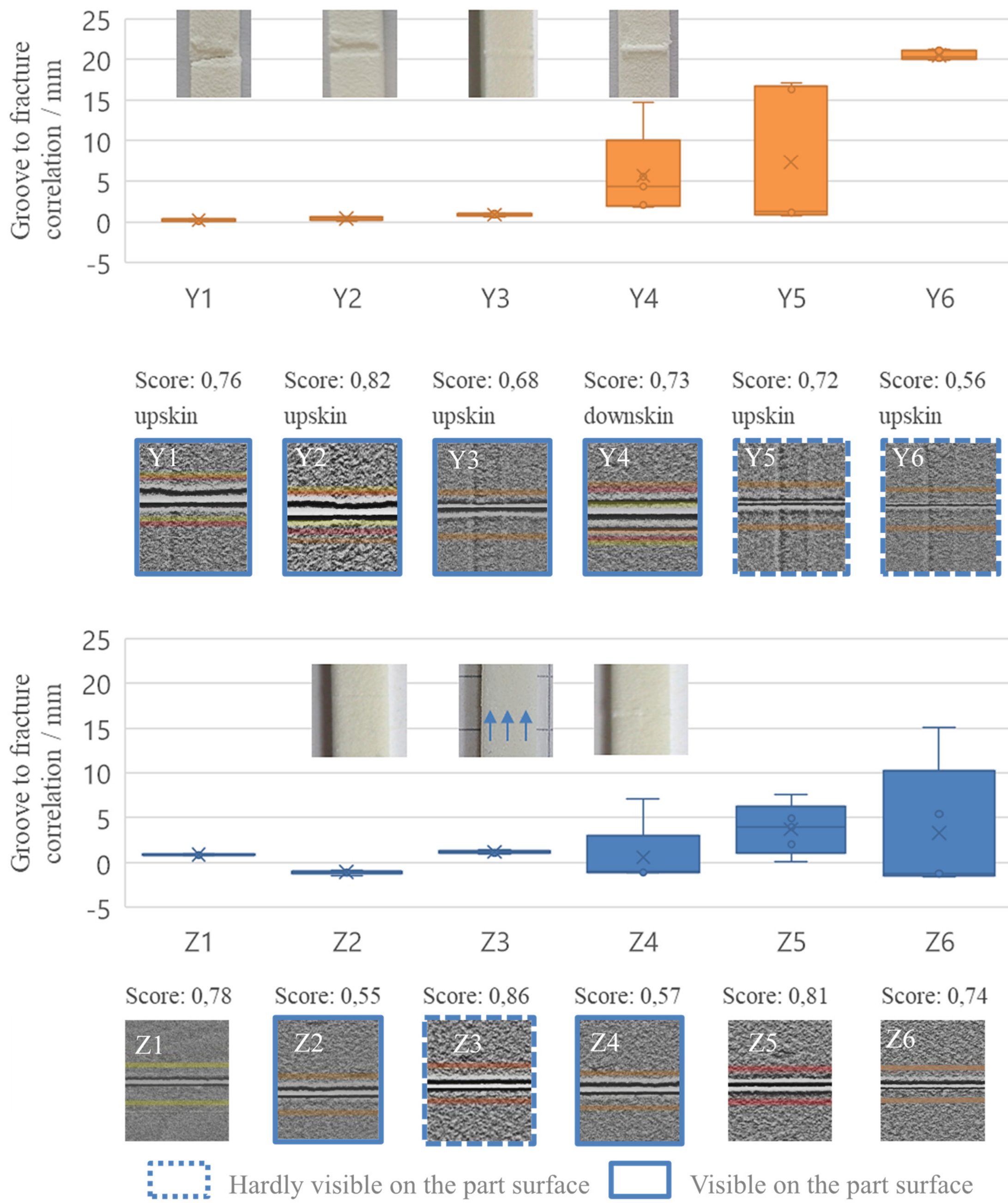

Figure 9 Correlation of the fracture and the powder bed flaw position for the build orientation Y-oriented and Z-oriented. For comparison the monitoring images as well as images of the grooves visible on the part surface are given

The Z oriented specimens do show good correlation and bad correlation without any direct link to the groove severity. Even the visibility on the part surface is not always an indicator for the failing position. In set Z1, no marks were found and in set Z3 only very light, hardly visible marks on the part surface can be seen. Still, those specimens were failing at the groove position, indicating some inner defects might be responsible for a stress concentration. The investigation with X-ray computer tomography is pending. The sets Z4-6 show a high variance in the fracture position, whereby Z5 is a very severe groove.

For the Y oriented specimens, the flaw position seems to be of importance. Therefore, comparable flaws have been applied to test sets at the position down skin, hence within the first layer of the part, in a mid-layer of the part and upskin in the very last layer of the parts. The correlation results are presented in Figure 10. For this test very severe grooves have been applied. For the upskin part, the powder bed flaw is visible on the part surface as dent, for the downskin parts a material elevation is visible. The mid part flaw is not visible on the part surface. Only for the upskin flaw set a correlation between the flaw and fracture position is possible.

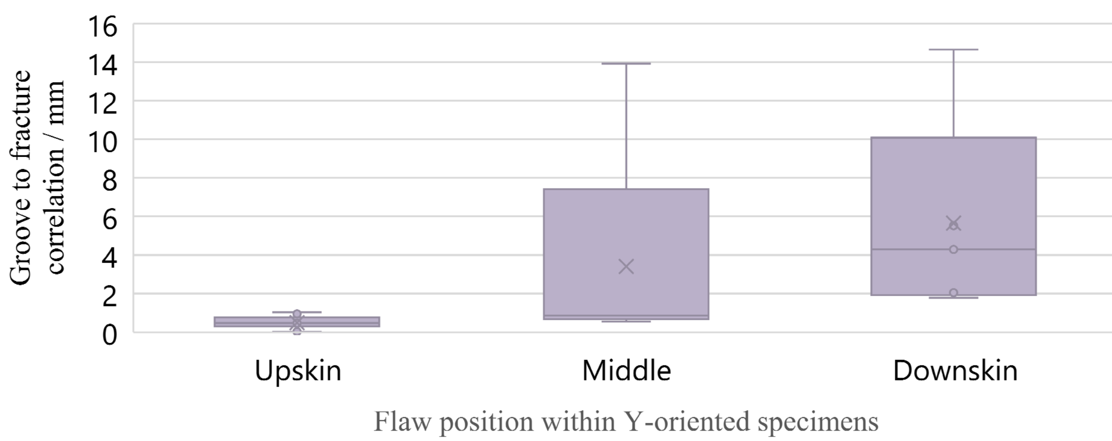

Figure 10 correlation of the fracture with grooves at different position within the test sets

It is assumed, that the flaw impacted parts and reference parts show the same mechanical properties. In Figure 11 and Figure 12 each flaw-reference pair is marked with a dot. Equal values would be positioned on the black line, representing the axis split. The color is given based on a visible defect on the part surface or no visible defects. If the fracture position and the groove position of the flaw specimen has shown a ±1,5 mm correlation, those points are marked with a black circle. Hence, all values below the axis split represent a pair of tensile test specimens where the dog bone with the applied flaw has a reduced elongation at break or tensile strength.

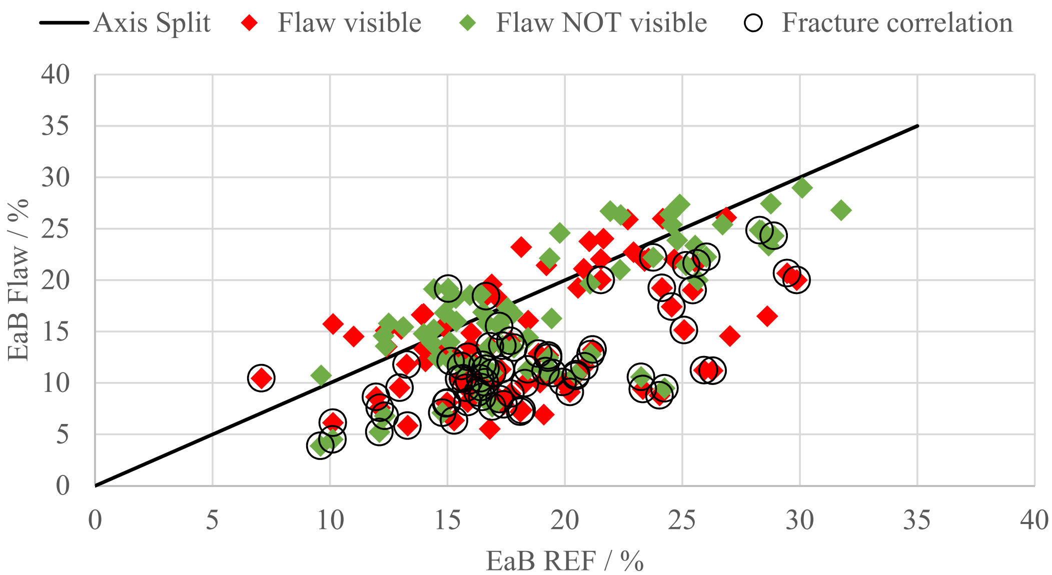

Figure 11 Comparison of the elongation at break (EaB) for reference (REF) and flaw specimens (each set is represented by one dot)

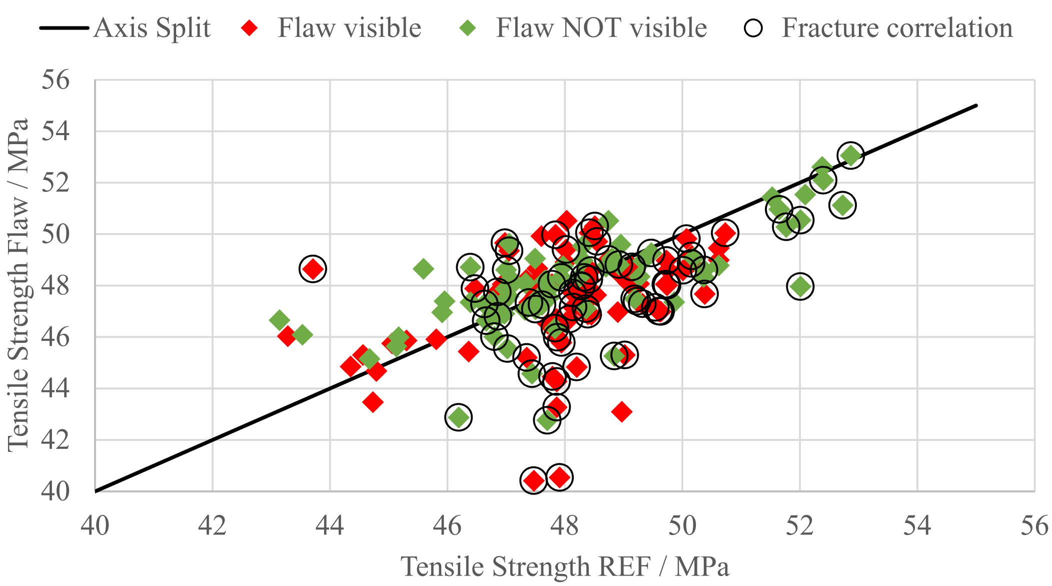

Figure 12 Comparison of the tensile strength for reference (REF) and flaw specimens (each set is represented by one dot)

Those diagrams show a reduction in the mechanical performance of the parts due to the applied artificial powder bed flaws, as most of the points are below the axis split. In relations, this can be described in percentage values, compare Table 1. Of all measured test sets, 73 % of the specimens with applied flaws do show a reduced elongation at break (EaB) while only 59 % show a reduced tensile strength (TS). This can be further distinguished for specimens built in Y and Z orientation, respectively.

Considering only the sets with good fracture-flaw correlation, 96 % of the parts showed a reduced EaB while only 78% showed reduced TS. But not all parts with visible marks show a groove fracture correlation. Here the percentage is decreased to 73 % of the parts, showing a reduced EaB compared to the reference part and 62 % for the TS.

Table 1 Percentage of weakened specimens due to the applied artificial powder spread flaws

Of all points (green plus red points below axis split)		EaB	TS
	all	73 %	59 %
	Y	66 %	51 %
	Z	78 %	64 %
With correlating flaw-fracture-position (black circle below axis split)			
	all	96 %	78 %
	Y	96 %	58 %
	Z	96 %	85 %
With visible marks on part surface (red points below axis split)			
	all	73 %	62 %
	Y	80 %	70 %
	Z	66 %	53 %

Summary, Discussion and Outlook

The artificially applied powder spread flaws are similar to the natural flaws, but do not mimic this type of powder spread imperfection entirely. The ridges, which are generated by the pin of the artificial flaw generator and which are not existing in natural flaws, might have an influence on the part performance. Up to now, this cannot be disproved. Still it is possible to create line flaws with adjustable intensity at various positions to the powder spread without disturbing the overall process. For each flawed specimen a reference specimen is positioned close by at a 4 mm part to part distance. All flawed and reference specimens were tested for elongation at break and tensile strength, as well as the fracture position were measured. For the flawed specimens the fracture position was compared with the groove position. For each set of flawed and reference specimens the fracture positions were checked, to exclude fracture at a specific position with other reasons than the groove itself.

Y oriented specimens with artificially applied grooves show a significant correlation between the fracture and groove position, if marks are visible on the part surface, which leads to stress concentration and subsequently to the fracture on this position. Hereby, the flaw position is very important, as the cross-section area is only reduced if the groove is within the last layer or layers of the part, thus ‘upskin’. In this test 20 % of the specimens do show visible marks but no reduced EaB. Thus, it is not implicated, that all parts with visible marks do have a fracture groove correlation or reduced mechanical properties.

Only one specimen in Y orientation has failed with a groove fracture correlation, without visible marks on the part surface. For this set a medium severe flaw was applied frequently every second layer, hence the investigation of single grooves or frequently applied grooves should be intensified in the future.

The Z oriented specimens with artificially applied grooves show no pattern related to the groove severity or the visibility of part surface defects. Fracture-Flaw correlation was obtained for medium severe grooves without visible marks, for severe grooves with visible marks and hardly visible marks on the part surface. However, a prediction on the part performance based on the flaw severity cannot be derived from the data so far, but based on the experiences the elongation at break and tensile strength reduction for the Z orientation is larger than for the Y orientation.

Up to now, the severity is only indicated by the monitoring system with changing the color of the bounding box, which represents a score given by the neuronal network on the expected quality of the prediction. If the score is high, the network is surer the prediction is correct, than with a low score. As sever flaws do show higher contrasts and might be easier to detect, this scoring works out most often. However, it is not perfect and should be used as brief indicator only. The groove severity scoring system shall be optimized in future.

As for several sets, grooves are visible on the part surface, it can be expected, that the melt viscosity is too high to smooth out the powder bed grooves applied by the plow pin. This is supported by images of the monitoring system, captured directly after the exposure process with open melt pools. Here, the grooves are still visible within the melt. This detail plus the measurements of Figure 9 indicate, that the melt surface is not completely flat. Hence the valleys or peaks of the powder spreading are still visible in the melt, resulting in a local variation of the volumetric energy density for the layer with the flaw as well as for the next layer, where the irregular surface will be leveled again. This applies only, if the groove is large enough.

As the artificial groove and the natural line flaw are limited in their comparability, more investigations based on natural grooves without ridges left and right of the flaw are required. Analyzing the variation of the energy density, based on increased or reduced layer thickness might lead to a better understanding, how flaws weaken the parts, if there is no obvious stress concentration due to visible marks and dents on the specimen surface.

The influence of line powder spread flaws is evident in the elongation at break, as a significant share of the specimens had shown reduced strain properties, if the fracture and flaw position are correlated. In percentage this is equal for both investigated build directions. The tensile strength is not influenced so much, as only 58 % of the Y oriented specimens showed reduced strength properties. For the Z orientation this is much more critical, as here 85 % of the specimens were measured with reduced strength compared to the reference specimen close by.

References

[1] S. Josupeit, S. Rüsenberg, and H.-J. Schmid, “A Material Based Quality Concept for Polymer Laser Sintering”, Proce. of the SFF Symposium, no. 24, pp. 44–54, 2013.

[2] S. Josupeit and H.-J. Schmid, “Thermal properties of polyamide 12 powder for application in laser sintering”, Internat. Congr. on Particle Technology (PARTEC), 2016.

[3] S. Josupeit, “On the Influence of Thermal Histories within Part Cakes on the Polymer Laser Sintering Process”, Dissertation, Universität Paderborn, Shaker Verlag, Paderborn, Germany, 2019.

[4] H. Klippstein and H.-J. Schmid, “Methodik zur Qualifizierung des Lasersinter Prozesses für die Serienfertigung”, in Rapid.Tech + FabCon 3.D International Hub for Additive Manufacturing, München, Carl Hanser Verlag GmbH & Co. KG, 2019, pp. 349–365.

[5] W. W. Wroe, J. Gladstone, T. Phillips, S. Fish, J. Beaman, and A. McElroy, “In-situ thermal image correlation with mechanical properties of nylon-12 in SLS”, Rapid Prototyping Journal, vol. 22, no. 5, pp. 794–800, 2016, doi: 10.1108/RPJ-10-2015-0158.

[6] Samantha Taylor, Joseph Beaman, and Scott Fish, “Thermal History Correlation with Mechanical Properties for Polymer Selective Laser Sintering (SLS)”, Solid Freeform Fabrication 2017: Proceedings of the 28th Annual International, pp. 1448–1463, 2017. Available: http://utw10945.utweb.utexas.edu/sites/default/files/2017/Manuscripts/ThermalHistoryCorrelationwithMechanicalProper.pdf

[7] S. H. Klippstein, F. Heiny, N. Pashikanti, M. Gessler, and H.-J. Schmid, “Powder Spread Process Monitoring in Polymer Laser Sintering and its Influences on Part Properties”, JOM, vol. 74, no. 3, pp. 1149–1157, 2022, doi: 10.1007/s11837-021-05042-w.